Electron Delocalization in Cross-Conjugated *p*-Phenylenevinylidene Oligomers

Mark Klokkenburg,[a] Martin Lutz,[b] Anthony L. Spek,[b] John H. van der Maas,[c] and Cornelis A. van Walree*[a]

Abstract: The synthesis, structure, and electronic properties of a series of cross-conjugated *p*-phenylenevinylidene oligomers with one to four double bonds are reported. The X-ray crystal structure of the compound with two double bonds reveals a nonplanar conformation with torsion angles about the C(phenylene)–C(vinylidene) and C(phenyl)–C(vinylidene) formal single bonds of 39.5(2)° and 30.5(2)°, respectively. Admixture of quinoid character in the ground state is observed. Infrared and Raman spectroscopy do not provide a clear picture of the degree of electron delocalization in the series, since the C=C stretching mode does not adequately reflect the C=C bond order and has a local nature. In contrast, electronic spectra and electrochemical data, as well as AM1 and PPP/SCF calculations, reveal that the cross-conjugated compounds basically behave as linearly π-conjugated systems in the sense that molecular orbitals are delocalized over the entire structure and systematically change in energy. The electronic interaction between the repeating units is, however, not very strong, which has the consequence that spatial extension of the molecular orbitals does not lead to a red shift of the highest occupied molecular orbital–lowest unoccupied molecular orbital (HOMO–LUMO) electronic transition. This is related to the feature that the modest narrowing of the HOMO–LUMO gap with the chain length is accompanied by a relatively large reduction of electron repulsion. This finding implies that care should be taken in the use of electronic spectra for the evaluation of conjugation phenomena.

Keywords: conjugation · cyclic voltammetry · semiempirical calculations · UV/Vis spectroscopy · vibrational spectroscopy

Introduction

An abundant amount of work has been directed towards the design of organic compounds and materials with attractive optical, optoelectronic, and conductive properties.[1] These properties have in common that they rest on the occurrence of electron delocalization. Linear π-conjugated systems, of which polyacetylene, poly(*p*-phenylenevinylene)s, and polythiophenes are well-known examples, have by far received the most attention. However, alternative modes of conjugation,[2, 3] such as σ conjugation found in polysilanes,[4] σ–π conjugation in oligo(cyclohexylidene)s[5, 6] and silylene-arylene polymers,[7, 8] and homoconjugation in diphenylpropanes, diphenylsilanes,[9, 10] and 7,7-diarylnorbornanes,[11] can also form the basis of interesting electronic features.

A form of conjugation which has only sparsely been addressed in materials research is cross-conjugation, which has been defined as the situation in which two unsaturated fragments are not conjugated to each other, but are both conjugated to a third unsaturated moiety.[12] Examples of simple cross-conjugated compounds are 3-methylene-1,4-pentadiene, benzophenone, and 1,1-diphenylethene. Recently, interest in this type of conjugation has flourished, as illustrated by the development of dendralene-based[13, 14] and enediyne-based[15–17] systems. This, however, does not alter the fact that the understanding of cross-conjugation is still limited. The principal question of how conjugated cross-conjugated compounds are, that is, to what extent electrons are delocalized in such systems, still needs a solid answer. In the few cases where a systematic set of compounds was available it was

[a] Dr. C. A. van Walree, M. Klokkenburg
Debye Institute
Department of Physical Organic Chemistry
Utrecht University
Padualaan 8, 3584 CH Utrecht (The Netherlands)
Fax: (+31) 302-534-533
E-mail: c.a.vanwalree@chem.uu.nl

[b] Dr. M. Lutz, Prof. A. L. Spek
Bijvoet Center for Biomolecular Research
Crystal and Structural Chemistry
Utrecht University
Padualaan 8, 3584 CH Utrecht (The Netherlands)

[c] Prof. J. H. van der Maas
Department of Vibrational Spectroscopy
Faculty of Chemistry
Utrecht University
Sorbonnelaan 16, 3584 CA Utrecht (The Netherlands)

DOI: 10.1002/chem.200204671

deduced that cross-conjugation does not result in pronounced π-electron delocalization and that electronic properties are essentially determined by the longest linear π-conjugated fragment present.[14, 18] These findings were, however, merely based on electronic absorption spectra and were not the result of a broad study.

In this contribution the synthesis and the characterization of cross-conjugated oligo(*p*-phenylenevinylidene)s **1**–**4**, a series of oligomers derived from 1,1-diphenylethene, are described. They are topological isomers of well-studied oligo(*p*-phenylenevinylene)s, the important difference being that the phenylene and phenyl moieties are connected by a single sp^2-hybridized carbon atom instead of by two sp^2-hybridized carbon atoms. Insight into the π-electron system of the oligo(*p*-phenylenevinylidene)s is obtained by the analysis of its properties as a function of chain length. Hereto IR, Raman, UV, and fluorescence spectroscopy are used, since the energy and intensity of characteristic transitions usually depend strongly on the extension of the π system. In addition, the electrochemical behavior of **1**–**3** is monitored by cyclic voltammetry, while a single-crystal X-ray structure of **2** could be obtained, through which the molecular structure is accurately established. The experimental results are correlated with PPP/SCF- and AM1-calculated properties. This study on oligo(*p*-phenylenevinylidene)s leads to new insights in the behavior of cross-conjugated compounds, insights which may lead to applications of cross-conjugated systems in materials science.

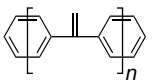

Results and Discussion

Synthesis: While 1,1-diphenylethene (**1**) was obtained from a commercial source, oligomers **2**–**4** were synthesized through a series of conversions involving the reaction between phenyllithium compounds and acetophenone derivatives, followed by dehydration of the formed alcohols (Scheme 1). For the synthesis of **2**, compound **5** was first prepared by treatment of 1,4-dilithiobenzene[19] with two equivalents of acetophenone in the presence of $CeCl_3$.[20, 21] Subsequent acid-catalyzed dehydration afforded **2**. Homologues **3** and **4** were synthesized in a procedure starting with the reaction between 4-bromophenyllithium and either 4-bromoacetophenone or 1,4-diacetylbenzene to give the respective products **6a** or **6b** in good yields (98%). Lithiation of **6a** and **6b** with three and four equivalents of *n*-butyllithium, respectively, followed by treatment with acetophenone resulted in **7a** and **7b**. Dehydration of **7a** and **7b** gave the oligomers **3** and **4**, respectively.

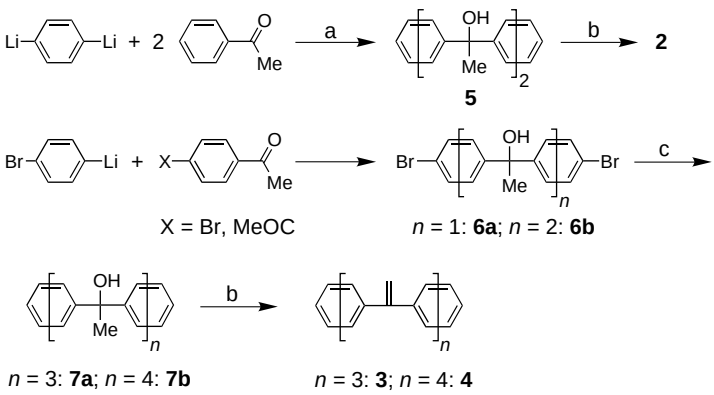

Scheme 1. Synthesis of oligo(*p*-phenylenevinylidene)s **1**–**4**. Reagents and conditions: a) $CeCl_3$; b) *p*-toluenesulfonic acid, toluene; c) BuLi (3 equiv for **6a**, 4 equiv for **6b**), acetophenone (2 equiv).

NMR analysis and GC-MS (after dehydration) showed that during the synthesis of alcohols **5**, **7a**, and **7b** a large number of compounds had been formed, including a substantial amount (30–40%) of aldol condensation products. Apparently, for dilithiocompounds nucleophilic addition is not particularly effective and these compounds also act as a base. In the synthesis of **5** cerium(III) chloride was used to favor nucleophilic addition and to suppress side reactions.[20, 21] Despite the strong oxophilicity of this reagent, this procedure did not result in a high yield.

Molecular structures: In the oligo(*p*-phenylenevinylidene)s rotation about the C(phenyl/phenylene)–C(vinylidene) formal single bonds is not free because of steric interactions between the ortho hydrogen atoms of neighboring aromatic groups. Therefore, for a given compound a number of geometries are possible which differ in the orientation of the vinylidene groups with respect to a phenylene moiety; these groups can be situated on either the same side or on different sides of the ring. Compound **2** can adopt either C_i or C_s symmetry, while **3** can occur in two different C_2 forms or in a C_1 form. Six structures are possible for **4**: two different isomers of C_i symmetry, two different isomers of C_s symmetry, and two different isomers of C_1 symmetry. Previous research has established that 1,1-diphenylethene (**1**) belongs to the C_2 point group.[22, 23]

In order to find out which structure prevails, **2** was subjected to single-crystal X-ray diffraction. This compound crystallizes in the orthorhombic Pbca space group with four molecules per unit cell. (See also the Experimental Section.) As depicted in Figure 1, the molecule has an exact, crystallographic C_i symmetry and thus adopts an undulating, stretched structure. (In the C_s geometry, with the two vinylidene groups occupying the same face of the phenylene ring, the structure is much more compact.) Although in the X-ray crystal structure the ortho hydrogen atoms H3 and H7 avoid each other, there are still close contacts between the hydrogen atoms on C5 and C11; the interatomic distance H5···H11 of 2.24 Å is significantly shorter than the sum of van der Waals radii of 2.40 Å. It is conspicuous that the torsion angles about the C(phenylene)–C(vinylidene) and the C(phenyl)–C(vinylidene) single bonds are different; the C1-C2-C4-C5 torsion angle is 39.5(2)°, while the C5-C4-C6-C11 angle amounts to 30.5(2)°. The nonplanar structure will reduce conjugation, but this disadvantage is not very severe since the overlap in a π system typically varies with the cosine of the torsion angle.

The olefinic C=C bond length, 1.329(2) Å (Table 1), is relatively short when compared to the average C=C bond length of 1.339(11) Å in "conjugated" (defined as having a torsion angle of 0–20° or 160–180°) phenyl-substituted

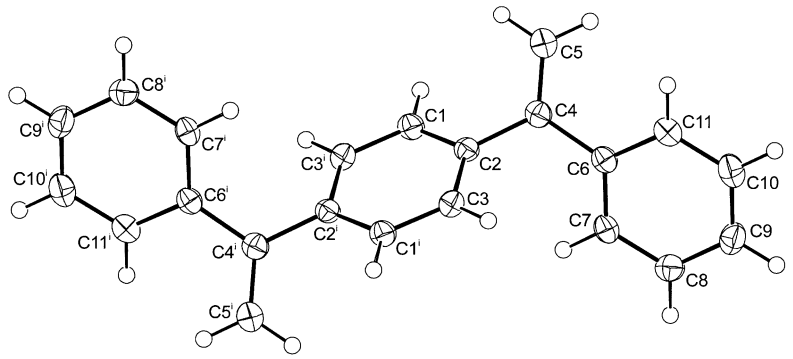

Figure 1. Displacement ellipsoid plot (50% probability) of the X-ray crystal structure of **2**. Symmetry operations i: $1-x, 2-y, -z$.

Table 1. C–C bond lengths in **2**.

Bond	Length [Å]	Bond	Length [Å]
C1–C2	1.396(2)	C1–C3^{i}	1.385(2)
C2–C3	1.395(2)	C2–C4	1.494(2)
C4–C5	1.329(2)	C4–C6	1.489(2)
C6–C7	1.395(2)	C6–C11	1.400(2)
C7–C8	1.390(2)	C8–C9	1.383(2)
C9–C10	1.381(2)	C10–C11	1.386(2)

alkenes.[24] Furthermore, the two formally single bonds C2–C4 and C4–C6, having respective lengths of 1.494(2) and 1.489(2) Å, belong to the long fraction of C(sp^2)–C(aryl) bonds, for which the average length is 1.470(15) Å.[24] From the bond lengths, the double bond in **2** thus seems to be rather isolated in comparison to planar π systems. It is however clear that delocalization is much more pronounced than in real isolated π systems. Although the bonds in the phenylene ring have normal lengths, the C1–C3^{i} distance is shorter than the C1–C2 and C2–C3 distances. This bond length alternation points to the admixture of some quinoid character in the ground state and must be based on a small degree of electron delocalization. Quinoid character is not observed for the outer phenyl rings, in which the C9–C10 and C8–C9 bonds are relatively short and the C6–C7 and C6–C11 bonds long. This suggests that electron delocalization is most pronounced in the central divinylbenzene-like unit.

To establish whether the crystal picked for the X-ray study was representative for the bulk of **2** as isolated, a powder X-ray pattern that was simulated from the single-crystal data was compared to a measured powder diffractogram (data not shown). The presence of a few weak lines in the experimental diffractogram which were not anticipated on basis of the simulation means that it is not possible to claim that the isolated material was 100% structurally homogeneous. There may be some C_s isomer present. We nevertheless believe that the highly prevailing geometry of **2** is the undulating stretched structure displayed in Figure 1.

AM1 calculations on compounds **1**–**3** were performed to investigate how molecular properties depend on the molecular geometry and on the chain length. Obtained heats of formations were 66.41 (**1**, C_2), 110.80 (**2**, C_i), 110.85 (**2**, C_s), 155.16 (**3**, C_2), 155.21 (**3**, C_1), and 155.22 (**3**, C_2') kcal mol^{-1}. These data show that all isomers of a given compound have an essentially identical heat of formation and that there is no thermodynamical driving force favoring the formation of only a single isomer. The presence of an excess of the C_i form of **2** may then be related to preferential crystallization or a to kinetic effect during the synthesis. The AM1 calculations also showed the orbital energies of isomers to be identical, which indicates that the degree of conjugation (see below) is independent of the actual molecular structure.

Structural features of the AM1 optimized structures were qualitatively in agreement with the X-ray crystal structure of **2**. All structures were twisted about the C(phenyl/phenylene)–C(vinylidene) single bonds by about 40°. Note that during the optimization the C(phenylene)–C(vinylidene) and C(phenyl)–C(vinylidene) torsion angles were constrained to be equal, so that the difference between them in the X-ray crystal structure of **2** could not be reproduced. In the AM1 structure of **1**, which was optimized without any restrictions, the torsion angle around the formal single bonds was however also close to 40°, which suggests that AM1 calculations give a value of 40° anyway. In line with the X-ray crystal structure, a small amount of quinoid character of the phenylene units is revealed; in all isomers of **2** and **3** the AM1-calculated "central" aromatic bonds lengths are 1.391–1.393 Å, while the other bonds are 1.402–1.403 Å long. In addition, in the phenyl groups the C–C bonds adjacent to the double bond are longer than the other bonds in that ring, which in their turn are not very different from each other.

Vibrational spectroscopy: The structural and conjugative properties of **1**–**4** were further investigated with IR and Raman spectroscopy. IR spectra of oligomers **2** and **3** are depicted in Figure 2, while Raman spectra of **1** and **4** are shown in Figure 3. The frequency of the most prominent signals along with their assignments[25–27] are compiled in Table 2. The following vibrations are of particular importance: the vinylidene C=C stretch mode near 1604 cm^{-1}, the ν_{12} breathing mode of the phenyl end groups at 998 cm^{-1}, the =CH_2 wag motion near 906 cm^{-1}, the *p*-phenylene C–H out-of-plane motion at 855 cm^{-1}, and the (monosubstituted) phenyl C–H out of plane mode near 775 cm^{-1}.

Although peak positions are very similar, the IR spectra of **2** and **3** are remarkably different (Figure 2). The spectrum of **2** contains sharp signals that give rise to speculation that **2** exists as a well-defined compound, that is, the C_i structure from Figure 1 must be very dominant. In contrast, the bands in the IR spectrum of **3** are broad (particularly in the interval 1300–950 cm^{-1}). To find out whether this was due to a structural inhomogeneity or to solid-state phenomena, IR spectra of solutions of **2** and **3** in chloroform were also recorded (not shown). In these spectra the bands of **2** and **3** were equally broad, a few bands occurred at different positions, and a few additional bands were present in the spectrum of **3**. Although

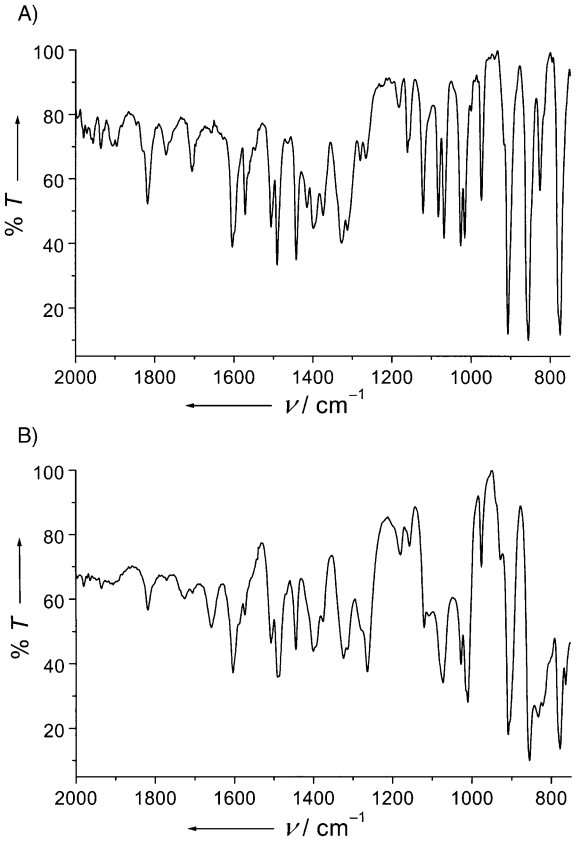

Figure 2. Infrared spectra of A) **2** and B) **3** in the frequency range 2000–750 cm^{-1}.

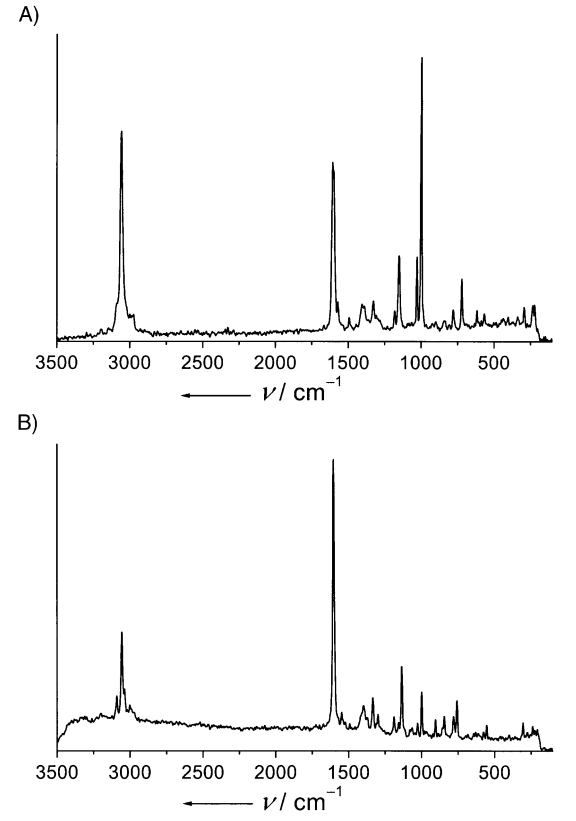

Figure 3. FT-Raman spectra of A) **1** and B) **4**.

Table 2. Compilation of most important infrared and Raman signals of oligomers **1**–**4**. All data are in cm^{-1}.

1		**2**		**3**		**4**		
IR	Raman	IR	Raman	IR	Raman	IR	Raman	Assignment[a]
3054	3058	3052	3057	3030	3056	3031	3056	ν C–H[b]
1609	1607	1604	1603	1603	1603	1603	1603	ν C=C[c]
1573		1571		1572		1572		ν_{8b}
1490		1490		1490		1491		ν_{19a}
1443		1441		1443		1443		ν_{19b}
1327		1327		1323		1323		ν_{14}
1026		1025		1026		1026		ν_{18a}
	998		998		997		998	ν_{12} monosubstituted
896		906		908		908		ω $=CH_2$
		855		855		854		γ C–H para-substituted
770		774		777		778		γ C–H monosubstituted

[a] ν: stretch mode; ω: wag mode; γ: out-of-plane bending mode. The numbers of stretch modes refer to benzene modes.[26] [b] The most intensive of a number of peaks. [c] Overlap with the ν_{8a} mode possible.

these observations might possibly be explained by a different point group of **3**, which possesses C_2 symmetry in the stretched structure, it is more probable that the broad signals of **3** in the solid state are caused by both solid-state phenomena and a structural heterogeneity. It can thus not be ruled out that, in addition to the stretched structure, other geometries are also present. Apart from intensity differences originating from a change of the number of phenyl end groups relative to the number of phenylene moieties, such as differences observed in the signals near 855 and 775 cm^{-1}, the IR spectrum of **4** (not shown) is very similar to that of **2**. This renders it likely that **4** also occurs mainly in the stretched C_i structure.

In both the IR and Raman spectra of **1**, the C=C stretch mode is found near 1607 cm^{-1}. This is a conspicuously low frequency as revealed by a comparison with data from compounds such as styrene (ν C=C = 1631 cm^{-1}),[27] α-methylstyrene (1630 cm^{-1}),[27] *cis*-stilbene (1629 cm^{-1}),[23, 28] *trans*-stilbene (1638 cm^{-1}), and related compounds.[29] The low frequency shows that the force constant of the C=C stretch motion is small, which can be tentatively interpreted to be a consequence of a considerably delocalized electron distribution in **1**.[22] However, AM1 calculations provide a different picture. In line with the experimental data, the (unscaled) 1,1-diphenylethene C=C stretch mode was calculated to be situated at a lower frequency than that of, for example, *trans*-stilbene (in which, in the optimized structure, the phenyl rings were rotated out of the C=C–H plane by 21.5°): 1853 versus 1877 cm^{-1}. Also, the AM1-calculated C=C stretch force constant in **1**, 7.28 mdyn $Å^{-1}$, is smaller than that in *trans*-stilbene, 7.59 mdyn $Å^{-1}$. Interestingly, these force constants are not consistent with the bond orders. In **1** these are 1.884 and 0.996 for the C=C bond and the adjacent formal single bonds, respectively. In *trans*-stilbene the corresponding bond orders were 1.845 and 1.030. The bond orders thus indicate that the C=C bond is stronger in **1** than in *trans*-stilbene, whereas the force constants indicate the opposite. This apparent discrepancy can be understood by considering the (π) bond order, p_{rs}, between two atoms r and s, which is defined as in Equation (1).

$$p_{rs} = \sum_i n_i c_{ri} c_{si} \quad (1)$$

Here c_{ri} and c_{si} represent the eigenvectors of r and s in the i^{th} molecular orbital, which is occupied by n_i electrons. According to Equation (1) the bond order reflects the number of electrons present at r and s; it does not however necessarily reflect the degree of bonding. This bonding appears to be less effective in **1** than in *trans*-stilbene, since the two C=C eigenvectors in the highest occupied molecular orbital (HOMO) in **1** (see Figure 6 below) are markedly different, whereas those in the HOMO of *trans*-stilbene are equal, giving rise to efficient overlap. The unequal π coefficients at the two C=C atoms in the HOMO of **1** are caused by the asymmetric substitution pattern. The eigenvector at the olefinic carbon atom bonded to the phenyl groups is much smaller because of the interaction with these groups. Hence, although the low C=C stretch frequency of **1** suggests that in the basic building block of the oligo(*p*-phenylenevinylidene)s strong electron delocalization between the double bond and the phenyl groups occurs, in reality the low frequency is the result of the asymmetric nature of the double bond. As far as we are aware, this is the first time that this low C=C stretch frequency of **1** has been rationalized in this way.

Table 2 shows that in both IR and Raman spectra, extension of the structure on going from **1** to **2** leads to a small shift of 4–5 cm^{-1} of the C=C stretch mode towards lower wavenumbers. Although one may be initially inclined to think that this reflects a small increase in electron delocalization, it is due rather to the fact that the vibrational spectra of **1** were obtained in the liquid phase and those of **2** in the solid phase. In the solid state (at 80 K) the C=C stretch mode of **1** is situated at 1604 cm^{-1} in the Raman spectrum and at 1606 cm^{-1} in the IR spectrum.[25] The $=CH_2$ wag frequency of **1** differs from that of **2** for the same reason; in the solid state it occurs at 905 cm^{-1}.[25] It then appears by inspection of Table 2 that throughout the whole series of compounds all major vibrations are found at essentially the same frequency. This implies that either the degree of conjugation does not change in going from **1** to **4** or that the frequencies of the vibrations are not susceptible to the degree of conjugation. The latter explanation would have the consequence that all vibrations taken into account, including the C=C stretch mode, have a local character. In this context it is noteworthy that only extremely small frequency shifts (particularly of the C=C stretch vibration) have been found in Raman data of oligomeric model compounds of poly(*p*-phenylenevinylene).[30, 31]

Since they reflect polarizability phenomena, Raman intensities are in principle better suited to probe conjugation phenomena than IR and Raman frequencies.[32] This concerns C=C stretching modes in particular. In Figure 4 the intensities of the C=C stretch signals, together with those of the C–H stretching mode, are plotted against the chain length. The intensities were normalized to the ν_{12} mode of the phenyl end groups, which represents the most appropriate reference signal. Starting at $n=2$ it is seen that the intensities of the C=C and C–H vibrations increase linearly with the number of vinylidene and phenylene groups. The steeper slope of the C=C signal obviously originates from the larger polarizability of this group. However, when the region between the origin and $n=2$ is considered, the relationship between the C=C intensity and n is superlinear.[33] This is exemplified by the feature that at $n=1$ the C=C intensity is lower than the C–H intensity. These observations suggest that the polarizability of the C=C bond changes appreciably in going from **1** to **2**, whereas upon moving to the longer compounds only additive effects are operative. Conjugation effects are thus only present when going from $n=1$ to $n=2$, the length at which the conjugation plateau seems to be reached already. This is however not in agreement with results presented below. Since the IR and Raman frequencies were also chain-length independent, it must be assumed that vibrations are local in nature. Since a similar conclusion was also drawn for *p*-phenylenevinylene oligomers,[34] this is likely to be true in general for conjugated materials incorporating phenylene units.

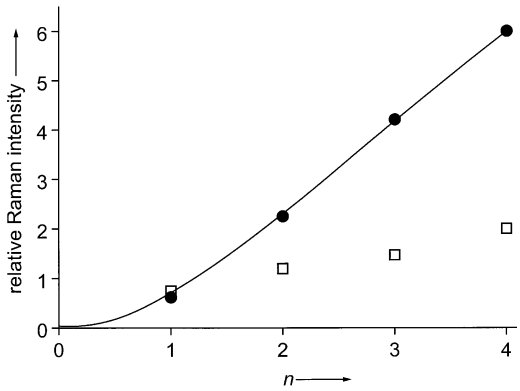

Figure 4. Relative intensities of the Raman C=C stretch mode at 1604 cm^{-1} (solid circles) and C–H stretch mode near 3060 cm^{-1} (open squares) of **1**–**4** as a function of chain length. Intensities were normalized to the ν_{12} mode of the phenyl groups at 997–998 cm^{-1} and were determined by measuring the peak height. The drawn line is a guide to the eye.

Cyclic voltammetry and orbital energies: To obtain information about the effect of the oligomer length on the redox properties and orbital energies, compounds **1**–**3** were studied by cyclic voltammetry. No cyclic voltammogram could be obtained for **4** owing to its poor solubility. As shown in Figure 5 for **1**, the oligomers display two highly irreversible oxidation waves, which correspond to the formation of the radical cation and the subsequent conversion into the

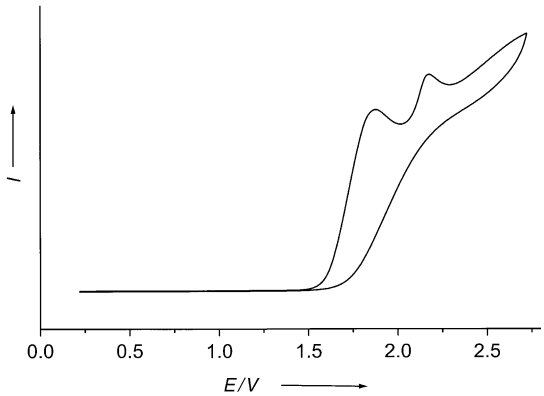

Figure 5. Cyclic voltammogram of 1,1-diphenylethene (**1**). The potential is given relative to the standard calomel electrode (SCE).

dication. Reduction processes were not observed in the available potential window.

As can be seen from Table 3, the first oxidation potential becomes lower with the oligomer length. This implies that the HOMO energy is raised and the radical cation becomes more stable as a function of chain length. It thus appears that the

Table 3. First and second oxidation potential (in V versus SCE) of oligomers **1**–**3** as determined by cyclic voltammetry.[a]

Compound	E_1^{ox}	E_2^{ox}
1	1.88[b]	2.17
2	1.72	1.90
3	1.67	1.8[c]

[a] Owing to the irreversibility of the oxidation processes, peak maxima are given as the potentials. [b] Value in agreement with literature data.[35] [c] Value could not be determined accurately because of low solubility.

oligo(*p*-phenylenevinylidene)s are conjugated in the sense that electron delocalization occurs upon chain elongation, thereby raising the HOMO level. The decrease in the first oxidation potentials is 0.16 and 0.05 V when going from **1** to **2** and from **2** to **3**, respectively. These steps are not as large as observed for linear π-conjugated compounds. For instance, for a series of phenyl end-capped oligothiophenes the first steps in oxidation potential with n are 0.28 and 0.18 V,[36] while for the reduction of oligo(*p*-phenylenevinylene)s the steps are 0.26 and 0.14 V.[37] The smaller step size indicates that the electronic interaction between building blocks in **1**–**3** is not as pronounced as in linear π-conjugated compounds. The second oxidation potential decreases with the chain length as well. In common with linear π-conjugated systems,[36–38] the decrease is faster than that of the first oxidation potential. Unfortunately, the limited number of data points did not allow a reliable determination of the coalescence point of the two oxidation processes.

The cyclic voltammetry results are supported by PPP/SCF and AM1 calculations. HOMO and lowest unoccupied molecular orbital (LUMO) plots of **1**–**3** obtained from the PPP calculations, along with the energies, are shown in Figure 6. It is important to mention that in all compounds the double bonds and aromatic rings together form a single delocalized system. However, the frontier orbitals are quite strongly localized on the double bonds. In particular the $=CH_2$ carbon atoms contribute appreciably. A similar pattern is exhibited by the frontier orbitals of dendralenes.[39] Also, the phases of the eigenvectors at the double bonds behave in exactly the same way as in dendralenes: in the HOMO the C=C units are π bonding but have an alternating phase with neighboring C=C units, and in the LUMO the "C=C" units are π antibonding while having the same phase as their neighbors. This makes it possible to regard oligo(*p*-phenylenevinylidene)s as dendralenes in which the double bonds are connected by phenylene spacers.

The PPP/SCF calculations nicely show that the HOMO is destabilized by chain extension, while the LUMO is stabilized by the same amount. However, as the chain becomes longer the effect is gradually dampened. When moving from **3** to **4** the difference is only 0.03 eV, which indicates that conjugation

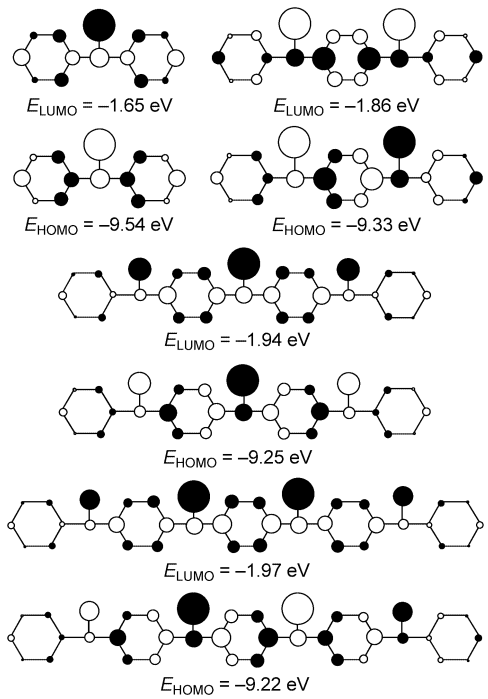

Figure 6. PPP/SCF-calculated HOMOs and LUMOs of compounds **1**–**4**, along with their energies. Circle radii are proportional to the size of coefficients.

is close to reaching its limit in the system with four double bonds. Not surprisingly, these observations are qualitatively reflected by the nature of the orbitals. The HOMOs and LUMOs have identical eigenvectors (there is only an additional nodal plane in the LUMO), and this accounts for the equal effect of chain extension on the HOMO and LUMO. In addition, the HOMOs and LUMOs tend to be localized in the center of the compounds. For **3** and **4** the contribution of p-type atomic orbitals in the terminal phenyl groups to the frontier orbitals is already small. This rationalizes the fact that attachment of another unit only has a limited effect.

The AM1 calculations yielded the same picture with regard to the orbital energies and constitutions as the PPP/SCF calculations. As an illustration, AM1 gave HOMO energies of −8.89, −8.69, and −8.62 eV and LUMO energies of −0.015, −0.21, and −0.28 eV for **1**, **2** (C_i), and **3** (C_2), respectively.

Electronic spectra: UV spectra of **1**–**4** are depicted in Figure 7, while maxima and absorption coefficients are compiled in Table 4. To provide insight into the spectra, PPP/SCF-calculated absorption maxima, oscillator strengths, and configuration interaction data are listed in Table 5. The results of these PPP calculations are in excellent agreement with the experimental data.

The spectra are complicated by the superposition of many transitions. For example, in line with previously reported calculations,[40] the PPP data point out that in the spectrum of **1** two forbidden transitions are situated at lower energy than the HOMO–LUMO transition. These transitions appear as the absorption onset in the region 270–295 nm. For the longer homologues these transitions are almost completely obscured by the HOMO–LUMO transition. Furthermore, the inter-

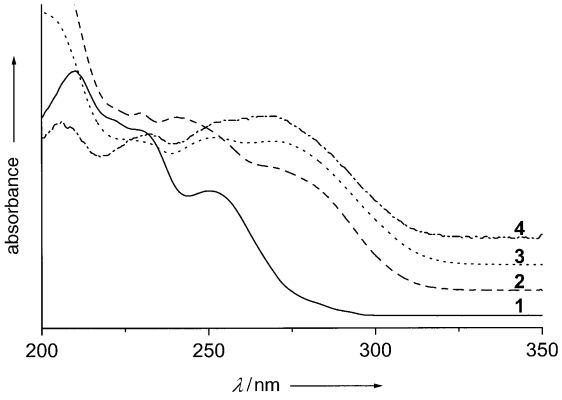

Figure 7. UV spectra of **1**–**4** in cyclohexane. Spectra were normalized at the low-energy maxima and were offset vertically in going from **1** to **4**. See Table 4 for absorption coefficients.

Table 4. Electronic absorption and fluorescence data for oligomers **1**–**4**.

	λ_{max}[a]	ε[b]	λ_{fl}[c]	Φ_{fl}[d]
1	292.5, 283.0, 256.0, 233.5	10.4	311[e]	0.0012
2	284.0, 271.0, 251.5, 240.0	18.5	336	0.0015
3	296.5, 272.0, 248.0	28.8	361	0.0016
4	271.5, 255[f]	–[g]	361	–[g]

[a] Absorption maxima in nm, determined from the second derivative spectrum. Only transitions at wavelengths higher than 230 nm are reported. [b] Absorption coefficient, in units of 10^3 м$^{-1}$cm^{-1}, at 250 (**1**) and 270 (**2**, **3**) nm. [c] Fluorescence maximum in nm. [d] Fluorescence quantum yield. [e] Corrected value, see Experimental Section. [f] Value subject to error because of limited signal-to-noise ratio. [g] Not determined due to limited solubility.

pretation of the spectra is complicated by a change in the sequence of orbitals and the different structures of the compounds. This is illustrated by the transition predominantly built up from the HOMO → LUMO + 1 (1–2′) and HOMO − 1 → LUMO (2–1′) excitations, which is forbidden for the C_i compounds **2** and **4**, but carries considerable oscillator strength in the C_2 species **1** and **3**. Nevertheless, in the present study the HOMO–LUMO transitions are of principal interest. They are found at 256 (**1**), 271 (**2**), 272 (**3**), and 271.5 (**4**) nm. This shows that there is a moderate red shift in going from **1** to **2**, whereas surprisingly no further change occurs when the number of repeating units increases. At first sight, this suggests that conjugation in the oligo(phenylenevinylidene) series **1**–**4** is limited to only two units. However, from the cyclic voltammetry data and the PPP-generated orbitals, it appeared that in the series **1**–**4** the HOMO and LUMO energies change until $n = 4$. It will be shown below that in this case the HOMO–LUMO transition energy is not a measure of the degree of conjugation. Stronger delocalization than anticipated from the UV maxima is also indicated by the intensity of the HOMO–LUMO transition, which is indicative of the occurrence of conjugation and which increases progressively with the chain length (Table 4).[41]

Fluorescence spectra of the oligomers initially show a red shift with increasing length (Figure 8, Table 4) but saturation is reached for compounds **3** and **4**. In other words, the first excited state of the long compounds is better stabilized. Furthermore, within the series there is a difference in the appearance of the fluorescence spectrum. Whereas the fluorescence spectrum of **1** is structureless, the spectra of the higher homologues exhibit a distinct vibrational splitting, which becomes more prominent with extension of the structure. From the approximate spacing of 1600 cm^{-1} it appears that the electronic transition is coupled to the C=C stretch vibration (compare with Table 2). This is in line with the large contribution of the C=C pπ orbitals to the HOMO and LUMO (Figure 6). It is noteworthy that under the structureless envelope of the emission of **1** a

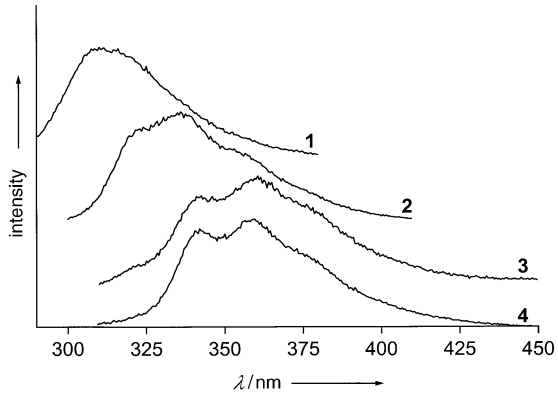

Figure 8. Fluorescence spectra of **1** (not corrected for the detector response) and **2**–**4** (corrected) in cyclohexane at room temperature.

Table 5. PPP/SCF-calculated electronic transitions of oligomers **1**–**4**.[a, b]

	λ [nm]	f	CI[c]
1	262	0.00	0.54(1–3′) + 0.54(3–1′) + 0.43(2–4′) + 0.43(4–2′)
	262	0.00	0.54(1–4′) + 0.54(4–1′) + 0.43(2–3′) + 0.43(3–2′)
	242	0.33	0.98(1–1′)
	226	0.51	0.69(1–2′) + 0.69(2–1′)
2	264	0.00	−0.62(1–6′) + 0.62(6–1′) − 0.28(3–6′) − 0.28(6–3′)
	256	0.61	0.94(1–1′)
	238	0.00	−0.68(1–2′) + 0.68(2–1′)
	231	0.85	0.63(2–2′) − 0.51(1–3′) + 0.51(3–1′)
3	255	0.91	0.92(1–1′) + 0.26(2–2′)
	253	0.47	0.66(1–2′) + 0.66(2–1′) + 0.24(1–4′) + 0.24(4–1′)
	235	0.27	0.61(2–2′) − 0.49(1–3′) + 0.49(3–1′)
	232	1.15	0.55(2–3′) − 0.55(3–2′) + 0.40(1–4′) + 0.40(4′–1)
4	255	1.15	0.87(1–1′) + 0.26(1–3′)
	254	0.00	−0.65(1–2′) + 0.65(2–1′)
	252	1.17	−0.61(2–2′) − 0.47(1–3′) + 0.47(1–3′) + 0.27(1–5′) − 0.27(5–1′)
	232	1.59	−0.50(3–3′) + 0.46(2–4′) + 0.46(4–2′) − 0.31(1–5′) + 0.31(5–1′)

[a] Calculations were run on geometries with torsion angles of 40° about the C–C single bonds. [b] Not all transitions of zero oscillator strength situated at lower wavelengths than the 1–1′ transition have been listed. [c] Configuration interaction coefficients larger than 0.20 are given.

vibrational substructure with spacing of 1600 cm^{-1} is hidden,[40] which shows that the fluorescence of this compound is associated with the LUMO–HOMO transition as well. In going to longer compounds in particular, the 0–0 emission gains intensity. This has been observed previously for linear π-conjugated oligomers,[36, 42] and it indicates that the (relaxed) S_1 geometry becomes more similar to the ground state. Thus, although the excited states of **3** and **4** were found to be situated at equal energies, they must be somewhat shifted along the C=C stretching coordinate with respect to each other.

Fluorescence quantum yields are low, of the order of 0.0015, and of comparable magnitude for all compounds. The latter observation supports the fact that for all compounds the same type of excited state is involved in the fluorescence process, despite the fact that in the absorption spectra several transitions were found to be situated closely together. The low values of the quantum yields strengthen the idea that the first excited state is localized at the olefinic bond(s), as excited states of alkenes are known to deactivate rapidly.

Correlation of HOMO–LUMO transitions and orbital energies: As described above, the HOMO–LUMO transition energies in the UV spectra seem to provide a different conjugation picture to that suggested by the HOMO and LUMO energies disclosed by cyclic voltammetry and PPP/SCF calculations. The orbital energies continue to change until $n = 4$, whereas in the UV spectrum saturation is already observed at $n = 2$. It should however be realized that in addition to being based on the HOMO–LUMO gap $\Delta E_{H\text{-}L}$, the energy of the singlet excited state formed upon HOMO–LUMO excitation, E_s, receives contributions from the Coulomb integral $J_{H\text{-}L}$ and the exchange integral $K_{H\text{-}L}$, according to Equation (2).[43]

$$E_s = \Delta E_{H\text{-}L} - J_{H\text{-}L} + 2K_{H\text{-}L} \quad (2)$$

The last two terms account for the decrease in repulsion energy when an electron is promoted from the HOMO to the LUMO. Data for **1**–**4**, extracted from the PPP/SCF calculations (see Experimental Section), are collected in Table 6. It is seen that the energy of the singlet state E_s decreases from **1** to **2**, but subsequently increases. As expected from the data in Figure 6, the HOMO–LUMO gap decreases continuously with *n*. The same trend is followed by the Coulomb and exchange integrals; this is in line with the expectation that in more extended systems the electronic repulsion is smaller. It now appears that within the series **1**–**4** the lowering of the excited state by narrowing of the band gap is opposed (and for the longer compounds, in fact, overcompensated for) by a decrease of the stabilizing effect of the Coulomb integral. The decrease of the exchange integral in its turn has a stabilizing contribution on the excited state, but this not sufficient to cancel the destabilizing effect of the Coulomb term. Hence, although the HOMO–LUMO gap decreases with the oligomer length, the HOMO–LUMO transition energy is not lowered since these molecular orbitals become more extended and electron repulsion is reduced. Recently, the Coulomb and exchange terms have been addressed to explain the chain-length dependence of the electronic spectra of electron donor–acceptor substituted *p*-phenylenevinylene oligomers.[44]

Table 6. Singlet energies E_s, energy gaps $\Delta E_{H\text{-}L}$, Coulomb integrals $J_{H\text{-}L}$, and exchange integrals $K_{H\text{-}L}$ of the HOMO–LUMO transition of oligomers **1**–**4** extracted from PPP/SCF calculations. Configuration interaction effects are not included. All data are in eV.

	E_S	$\Delta E_{H\text{-}L}$	$J_{H\text{-}L}$	$K_{H\text{-}L}$
1	5.22	7.89	4.49	0.91
2	5.01	7.47	3.75	0.65
3	5.08	7.31	3.27	0.52
4	5.18	7.25	2.93	0.43

The situation outlined in the last paragraph has some important consequences. Firstly, despite being very frequently applied as a measure of the HOMO–LUMO gap and the extent of conjugation of a system, electronic spectra are not unambiguous in this use. This should also hold for linear π-conjugated systems, in which the Coulomb integral must also decrease with the chain length. However, here the reduction of the HOMO–LUMO gap with *n* is usually much stronger, so that the role of the Coulomb term is less prominent. Nevertheless, in a given system it is more appropriate to consider the HOMO and LUMO energies to assess the extent of conjugation. Secondly, the quite unique situation exists in cross-conjugated materials that extension of the conjugated system is not accompanied by a bathochromic shift of the optical transition. Although it may be premature to state that is true for all cross-conjugated systems, we note that chain extension in dendralene-type compounds also leads to changes in redox potentials but not to significant UV/Vis shifts.[14, 18]

Conclusion

It has not been easy to obtain a coherent view on the degree of electron delocalization in oligo(*p*-phenylenevinylidene)s **1**–**4**, since techniques which are frequently applied for the evaluation of conjugation effects do not provide unequivocal information. For instance, whereas the low frequency of the C=C stretch mode in **1** suggests that electrons in the double bonds are strongly delocalized, this frequency is actually due to the asymmetric substitution pattern. When studied as a function of the oligomer length neither vibrational peak positions nor intensities give a reliable picture, since modes have a local character. Moreover, UV spectra can be interpreted by the conjugation effectively reaching its limit at $n = 2$, but in reality they indicate that the decrease of the HOMO–LUMO gap is accompanied by a relatively strong reduction in electron repulsion.

Despite the fact that the spectroscopic data should be treated with some caution, they clearly reveal that the largest changes in the series occur when going from **1** to **2**. In this step, a pronounced red shift of the UV and fluorescence maxima takes place, and a superlinear increase of the C=C Raman intensity is found. These results point at a substantial extension of the delocalized system. In this connection it should be realized that **2** can be considered as consisting of a

central phenylene group with two linearly π-conjugated double bonds attached; it is somewhat reminiscent of divinylbenzene. This is also suggested by the X-ray crystal structure of **2**, in which quinoid character is only present in the phenylene ring and not in the outer phenyl groups. Consequently, in common with other systems,[14, 18, 45] electron delocalization by linear π conjugation is favored over delocalization by cross-conjugation.

Nevertheless, in the complete series **1**–**4** conjugation extends beyond the divinylbenzene moiety. This is substantiated by a number of features. The frontier molecular orbitals are delocalized over the entire structure, although they have the largest contributions from the central part of the compounds. Simultaneously the HOMO and LUMO energies vary systematically with the chain length; this is supported by the oxidation potentials. Furthermore, the AM1 data suggest a small degree of quinoid character to be present in all phenylene moieties of the longer compounds. Thus, in general, the electronic system of oligo(*p*-phenylenevinylidene)s resembles that of linear π-conjugated oligomers. However, in a quantitative sense conjugation is moderate and the electronic interaction between repeating units is not very strong. In the longest homologue **4**, which contains only four double bonds, the electron delocalization is already close to its limits. The change of the HOMO and LUMO levels with *n* is quite small, so that the reduction of electron repulsion is relatively strong and optical transitions are virtually chain-length independent. In this connection it is worth mentioning that a theoretical model showed that among all acyclic π systems the 1,1-disubstituted ethene topology leads to a maximal HOMO–LUMO gap.[39] The feature that the extension of the conjugated system is not accompanied by a bathochromic shift of electronic transitions renders cross-conjugated materials interesting candidates for optoelectronic applications that rely on transparency in the visible region, such as nonlinear optical materials.

A final point to be addressed is how far properties of the oligo(*p*-phenylenevinylidene)s are representative for other types of cross-conjugated compounds. On one hand, based on other reports dealing with electronic properties of cross-conjugated compounds, which generally also fail to exhibit strong shifts of HOMO–LUMO transitions,[12, 14, 18] we are inclined to think that most cross-conjugated systems behave similarly to oligo(*p*-phenylenevinylidene)s. On the other hand, it should be realized that there are two factors which have an unfavorable effect on the conjugation in oligo(*p*-phenylenevinylidene)s. These are the nonplanar structure[46] and the high resonance energy of the incorporated aromatic moieties.[38] Although, for instance, dendralenes are also not planar,[47] somewhat stronger interactions may be expected for other classes of cross-conjugated systems.

Experimental Section

General: NMR spectra were recorded on Bruker AC 300 or Varian Unity Inova spectrometers (both operating at 300 MHz for ^{1}H and 75 MHz for ^{13}C NMR spectroscopy). Chemical shifts are given in ppm relative to internal tetramethylsilane. Melting points were determined on a Mettler FP5/FP51 photoelectric apparatus. HPLC was performed by using a Hypersil ODS (c18) 5u column in combination with a Thermo Separation Products Series 200 pump and UV detector (monitoring at 264 nm). For gas chromatography a Varian 3400 gas chromatograph equipped with a DB5 capillary column was used. GC-MS spectra were collected on an ATI UNICAM Automass System 2 quadropole mass spectrometer (electron ionization (EI), 70 eV), while probe-analysis mass spectra were obtained on a Jeol JMS-AX505W mass spectrometer (EI). Elemental analysis was carried out at Kolbe Microanalytisches Laboratorium in Mülheim an der Ruhr, Germany.

UV/Vis spectra were recorded on a Varian Cary 1 UV-Vis or a Varian Cary 5 UV/Vis-NIR spectrophotometer. Fluorescence spectra were obtained by using a Spex fluorolog instrument, with excitation wavelengths of 250, 265, 265, and 267 nm for compounds **1**, **2**, **3**, and **4**, respectively. Emission spectra were corrected for the spectral response of the detector by the use of a correction factor file provided by the manufacturer. Since this file does not cover wavelengths below 300 nm, the fluorescence emission spectrum of **1** was not corrected. Correction of part of the spectrum gave a maximum of 311 nm. Fluorescence quantum yields[48] were determined with naphthalene in cyclohexane ($\Phi_{fl} = 0.23$) as the reference. Solutions were purged with argon for at least ten minutes. When necessary, fluorescence samples were purified by HPLC. Both UV-Vis and fluorescence spectra were recorded in spectrophotometric-grade cyclohexane (Acros). Cyclic voltammetry measurements were performed by using an EG&G Princeton Applied Research Model 263A potentiostat/galvanostat at a scan rate of 50 mV s^{-1}. Solutions of **1**–**3** (< 0.5 g L^{-1}) in acetonitrile (freshly distilled from CaH_2) were used, with 0.1 M anhydrous tetrabutylammonium hexafluorophosphate (Fluka, electrochemical grade) as the electrolyte. Prior to measurement, the solution was purged with nitrogen for at least ten minutes. Oxidation potentials were measured relative to a $Ag/AgNO_3$ (0.1 M) electrode, with Pt working and counter electrodes. By determining the potential of the ferrocene/ferrocinium couple ($E_{1/2} = +0.31$ V versus SCE), oxidation potentials were calibrated to the SCE electrode. Since we were primarily interested in the variation of the electrochemical behavior within the series **1**–**4**, peak values of the irreversible waves were taken as the oxidation potential. IR spectra were measured on a Perkin Elmer 2000 FT-IR spectrometer, operating with medium apodization at 4 cm^{-1} spectral resolution, in combination with a Golden Gate Single Reflection Diamond ATR system. FT-Raman spectra were recorded with a Perkin Elmer System 2000 NIR FT-Raman spectrometer equipped with a Nd:YAG laser (1064 nm) and an InGaAs detector. The Raman spectra were collected with a laser power of 300 mW at medium apodization and a spectral resolution of 4 cm^{-1}. The IR and Raman spectra were averaged from 16 scans.

Calculations: PPP/SCF/CI calculations were performed with a home-adapted version of Griffiths' program.[49] Torsion angles of 40° around the C–C formal single bonds were introduced by correction of the bond resonance energy with cos40°. For **1** a full configuration interaction was performed, while for the other compounds the configuration interaction included states arising from excitations from any of the six highest occupied to any of the six lowest unoccupied levels. Exchange integrals *K* and Coulomb integrals *J* were obtained by use of Equation (2) and Equation (3) in which E_T is the energy of the triplet state.

$$2K = E_S - E_T \quad (3)$$

AM1 calculations were run with the MOPAC7 package.[50] Geometries were optimized with the eigenvector-following routine. In order to obtain the desired symmetry, symmetry relations were imposed on the dihedral angles around the C(phenyl/phenylene)–C(vinylidene) single bonds. Force calculations were run to establish that the obtained geometries were minima on the potential energy surface and to calculate vibrational spectra.

X-ray crystallography: X-ray intensities were collected on a Nonius KappaCCD diffractometer with rotating anode and $Mo_{K\alpha}$ radiation (graphite monochromator, $\lambda = 0.71073$ Å). An absorption correction was not considered necessary. The reflections were merged by using the program SORTAV.[51] The structure was solved with direct methods by using the program SIR97[52] and refined with the program SHELXL[53] against F^2 of all reflections. Non-hydrogen atoms were refined freely with anisotropic displacement parameters. All hydrogen atoms were located in the difference Fourier map and were refined as rigid groups. The drawings,

structure calculations, and checking for higher symmetry were performed with the program PLATON.[54] Crystal data and experimental details are listed in Table 7. CCDC-198762 contains the supplementary crystallographic data for this paper. These data can be obtained free of charge via www.ccdc.cam.ac.uk/conts/retrieving.html (or from the Cambridge Crystallographic Data Centre, 12 Union Road, Cambridge CB2 1EZ, UK; fax: (+44) 1223-336033; or deposit@ccdc.cam.ac.uk).

Table 7. Crystal data for **2** and experimental details.

formula	$C_{22}H_{18}$
formula weight	282.36
crystal system	orthorhombic
space group	Pbca (no. 61)
a [Å]	10.7113(3)
b [Å]	7.4158(2)
c [Å]	19.3568(6)
V [Å]	1537.57(8)
Z	4
ρ [g cm^{-3}]	1.220
μ (Mo-K$_\alpha$) [mm^{-1}]	0.069
$F(000)$	600
crystal size [mm]	$0.03 \times 0.12 \times 0.30$
data collection:	
T [K]	150
θ_{min}, θ_{max} [°]	2.1, 23.5
data set (h, k, l)	0:11, 0:8, 0:21
measured data	14846
unique data	1130 ($R_{int} = 0.075$)
observed data [$I > 2\sigma(I)$]	845
refinement:	
no. of parameters	100
weighting scheme [w^{-1}]	$\sigma^2(F_0^2) + (0.0594P)^2$
R_1,[a] wR_2[b] (obs. refl.)	0.0381, 0.0882
R_1, wR_2 (all refl.)	0.0607, 0.0996
S	1.080
Min. and max. residual densities [e A^{-3}]	−0.20, 0.13

[a] $R_1 = \Sigma||F_0| - |F_c||/\Sigma|F_0|$. [b] $wR_2 = [\Sigma[w(F_0^2 - F_c^2)^2]/\Sigma(w(F_0^2)^2)]^{1/2}$.

Synthesis: All reactions involving organolithium compounds were performed in a dry nitrogen atmosphere. Diethyl ether, tetrahydrofuran (THF), and toluene were distilled from sodium benzophenone prior to use. Silica (Acros, 0.035–0.070 nm, pore diameter approximately 6 nm) was used to carry out column chromatography. The purity of compounds was established by thin-layer chromatography (Merck 60 F254 silicagel), IR spectroscopy, ^{1}H and ^{13}C NMR spectroscopy, and HPLC (with methanol as the eluent). 1,2-Diphenylethene (**1**) was obtained from Acros (99%) and used as received. Commercially available reagents were used without further purification.

1,4-Bis(1-phenylvinyl)benzene (2): Firstly, 1,4-dilithiobenzene was prepared according to a modification of the procedure described by Brandsma and Verkruijsse.[19] In a two-necked round-bottomed flask 1,4-dibromobenzene (2.10 g, 8.90 mmol) was dissolved in THF (40 mL). The stirred solution was cooled to −60 °C and *n*-butyllithium in *n*-hexane (13.1 mL of a 1.42 M solution, 18.6 mmol) was added over 10 min. After 2 h a cold (−60 °C), dry suspension of $CeCl_3$ (6.56 g, 26.7 mmol) in THF was added to the white suspension. The reaction mixture was stirred for 1 h at −60 °C, after which a solution of acetophenone (2.14 g, 17.8 mmol) in THF (10 mL) was introduced over 5 min. The mixture was allowed to warm to room temperature overnight and was poured into water (200 mL). The aqueous system was extracted with diethyl ether (4×100 mL) after which the combined organic layers were washed with water (100 mL), dried over $MgSO_4$, and filtered. Evaporation of the solvent left the yellow solid **5**, which was not pure and was not fully characterized. The crude **5** was dissolved in toluene (150 mL) and placed in a Dean-Stark apparatus. A catalytic amount of *p*-toluenesulfonic acid was added and the mixture was boiled for 12 h. Evaporation of the toluene at reduced pressure left a yellow solid, which proved to be a mixture of products. Compound **2** was isolated by column chromatography (with chloroform as the eluent) and further purified by crystallization from methanol (100 mL) at −20 °C. Compound **2** was obtained as an off-white solid (0.14 g, 0.50 mmol, 6%); m.p. 135 °C (lit.:[55] 123–124, 131.5, or 138 °C); ^{1}H NMR ($CDCl_3$): $\delta = 7.40$–7.32 (m, 10H; Ar-H), 7.31 (s, 4H; Ar-H), 5.51 (d, $^2J(H,H) = 1.2$ Hz, 2H; =CH_2), 5.46 (d, $^2J(H,H) = 1.2$ Hz, 2H; =CH_2) ppm; ^{13}C NMR ($CDCl_3$): $\delta = 149.7$ (*C*=CH_2), 141.4, 140.8, 128.3, 128.2, 128.0, 127.7, 114.2 (C=*C*H$_2$) ppm; IR: $\tilde{\nu} = 3092$, 3052, 1818, 1604, 1571, 1506, 1490, 1441, 1327, 1025, 906, 855, 774 cm^{-1}; GC-MS (EI): m/z: 282 [M$^+$].

1,1-Bis(4-bromophenyl)ethanol (6a): A solution of 1,4-dibromobenzene (3.00 g, 12.7 mmol) in diethyl ether (50 mL) was placed in a two-necked round-bottomed flask. *n*-Butyllithium in *n*-hexane (7.9 mL of a 1.60 M solution, 12.6 mmol) was added over 10 min. After 30 min, a solution of 4-bromoacetophenone (2.53 g, 12.7 mmol) in diethyl ether (20 mL) was introduced. Subsequently the reaction mixture was stirred for 12 h at room temperature. The solution was poured into water (200 mL), the layers were separated, and the water layer was extracted with diethyl ether (4×75 mL). The combined organic layers were washed with water (100 mL), dried on $MgSO_4$, filtered, and evaporated to dryness. Purity was 95% (GC); further purification was not considered necessary. Compound **6a** was obtained as a yellow solid (4.43 g, 12.4 mmol, 98%); m.p. 76 °C; ^{1}H NMR ($CDCl_3$): $\delta = 7.44$, 7.26 (AA′BB′, $^3J(H,H) = 8.7$ Hz, 2×4H; Ar-H), 2.12 (s, 1H; OH), 1.90 (s, 3H; Me) ppm; ^{13}C NMR ($CDCl_3$): $\delta = 146.5$, 131.4, 127.6, 121.3, 75.6 (C–OH), 30.7 (Me) ppm; IR: $\tilde{\nu} = 3563$, 2976, 2928, 1904, 1678, 1590, 1483, 1398, 1076, 1007, 916, 833 cm^{-1}.

1,1-Bis[4-(1-phenylvinyl)phenyl]ethene (3): Compound **6a** (2.49 g, 7.00 mmol) was dissolved in diethyl ether (60 mL) and placed in a two-necked round-bottomed flask. This mixture was stirred and *n*-butyllithium in *n*-hexane (14.5 mL of a 1.6 M solution, 23.2 mmol) was added over 15 min. Stirring was continued and after 1.5 h a solution of acetophenone (2.8 g, 23.1 mmol) in diethyl ether (30 mL) was slowly introduced to the white suspension. The mixture was stirred for an additional 12 h at room temperature and poured into water (200 mL). The water layer was extracted with diethyl ether (4×75 mL). The combined organic layers were washed with water (100 mL), dried over $MgSO_4$, and filtered. Evaporation of the solvent left a yellow solid, **7a**. This compound was dehydrated by the procedure described for **2**. Evaporation of the solvent at reduced pressure yielded a mixture of products. Volatile components were removed by kugelrohr distillation (0.04 mbar, 50–180 °C). The residue was further purified by column chromatography (with hexane/$CHCl_3$ (1:1) as the eluent). Compound **3** was obtained as a yellowish solid (0.23 g, 0.60 mmol, 9%); m.p. 165 °C; ^{1}H NMR ($CDCl_3$): $\delta = 7.37$–7.34 (18H, m; Ar-H), 5.51 (d, $^2J(H,H) = 1.2$ Hz, 2H; =CH_2), 5.50 (s, 2H; central =CH_2), 5.47 (d, $^2J(H,H) = 1.2$ Hz, 2H; =CH_2) ppm; ^{13}C NMR ($CDCl_3$): $\delta = 149.7$ (*C*=CH_2), 149.4 (*C*=CH_2), 141.4, 140.9, 140.8, 128.3, 128.2, 128.1, 128.0, 127.8, 114.3 (C=*C*H$_2$) ppm; IR: $\tilde{\nu} = 3030$, 1818, 1658, 1603, 1572, 1507, 1490, 1443, 1400, 1323, 1263, 1072, 1026, 1009, 908, 855, 777 cm^{-1}; GC-MS (EI): m/z: 384 [M$^+$]; elemental analysis: calcd (%) for $C_{30}H_{24}$ (384.5): C 93.71, H 6.29; found: C 93.58, H 6.22.

1,4-Bis[1-hydroxy-1-(4-bromophenyl)ethyl]benzene (6b): This compound was prepared from 1,4-dibromobenzene (5.00 g, 21.2 mmol), *n*-butyllithium in *n*-hexane (13.2 mL of a 1.6 M solution, 21.1 mmol), and 1,4-diacetylbenzene (1.72 g, 10.6 mmol in diethyl ether/THF (8:2)) as described for **6a**. Compound **6b** was obtained as a brown solid (purity 91% by GC) in quantitative yield; m.p. 130 °C; ^{1}H NMR ($CDCl_3$): $\delta = 7.43$, 7.25 (AA′BB′, $^3J(H,H) = 8.9$ Hz, 2×4H; Ar-H), 7.31 (s, 4H; Ar-H), 2.32 (s, 2H; OH), 1.89 (s, 6H; Me) ppm; ^{13}C NMR ($CDCl_3$): $\delta = 146.9$, 146.3, 131.2, 127.6, 125.7, 121.3, 75.6 (C–OH), 30.7 (Me) ppm; IR: $\tilde{\nu} = 3426$ (O–H), 2976, 1676, 1507, 1076, 1008, 1016, 827 cm^{-1}.

1,4-Bis{1-[4-(1-phenylvinyl)phenyl]vinyl}benzene (4): First, **7b** was prepared from **6b** (0.40 g, 0.84 mmol), *n*-butyllithium in *n*-hexane (2 mL of a 1.6 M solution, 3.2 mmol), and acetophenone (0.29 g, 2.4 mmol) as described above for **7a**. The impure **7b** was not completely characterized. Crude **7b** was dehydrated as described before. After evaporation of the solvent at reduced pressure a mixture of products was obtained, from which volatile components were removed by kugelrohr distillation (0.04 mbar, 50–190 °C). The residue was further purified by column chromatography (with hexane/chloroform (3:7) as the eluent). Compound **4** was obtained as a white solid (27.4 mg, 0.056 mmol, 7%); m.p. 211 °C; ^{1}H NMR ($CDCl_3$): $\delta = 7.37$–7.33 (22H, m; Ar-H), 5.51 (m, 6H; =CH_2), 5.47 (d, $^2J(H,H) = 1.1$ Hz, 2H; =CH_2) ppm; IR: $\tilde{\nu} = 3031$, 1817, 1603, 1572, 1505, 1491, 1443, 1400, 1323, 1119, 1073, 1026, 1014, 908, 854, 778 cm^{-1}; MS (EI): m/z: 486 [M$^+$].

The solubility of **4** was too low to record a ^{13}C NMR spectrum of satisfactory signal-to-noise ratio.

Acknowledgement

The authors thank A. Schouten for recording a powder X-ray diffraction pattern and Prof. L. W. Jenneskens and Dr. T. Visser for fruitful discussions. This work was supported in part (M.L., A.L.S.) by the Council for Chemical Sciences of the Netherlands Organization for Scientific Research (CW-NWO).

[1] *Handbook of Conducting Polymers*, 2nd ed. (Eds.: T. A. Skotheim, R. L. Elsenbaumer, J. R. Reynolds), Marcel Dekker, New York, **1998**.
[2] M. J. S. Dewar, in *Modern Models of Bonding and Delocalization* (Eds.: J. F. Liebman, A. Greenberg), VCH, Weinheim, **1988**, pp. 2 – 61.
[3] S. Winstein, *Spec. Publ. Chem. Soc.* **1967**, *21*, 5 – 45.
[4] R. D. Miller, J. Michl, *Chem. Rev.* **1989**, *89*, 1359 – 1410.
[5] F. J. Hoogesteger, C. A. van Walree, L. W. Jenneskens, M. R. Roest, J. W. Verhoeven, W. Schuddeboom, J. J. Piet, J. M. Warman, *Chem. Eur. J.* **2000**, *6*, 2948 – 2959.
[6] E. P. A. M. Bakkers, A. W. Marsman, L. W. Jenneskens, D. Vanmaekelbergh, *Angew. Chem.* **2000**, *112*, 2385 – 2388; *Angew. Chem. Int. Ed.* **2000**, *39*, 2297 – 2299.
[7] M.-C. Fang, A. Watanabe, M. Matsuda, *Macromolecules* **1996**, *29*, 6807 – 6813.
[8] G. Kwak, T. Masuda, *Macromolecules* **2002**, *35*, 4138 – 4142.
[9] C. A. van Walree, H. Kooijman, A. L. Spek, J. W. Zwikker, L. W. Jenneskens, *J. Chem. Soc. Chem. Commun.* **1995**, 35 – 36.
[10] C. A. van Walree, M. R. Roest, W. Schuddeboom, L. W. Jenneskens, J. W. Verhoeven, J. M. Warman, H. Kooijman, A. L. Spek, *J. Am. Chem. Soc.* **1996**, *118*, 8395 – 8407.
[11] A. García Martínez, J. Osío Barcina, A. de Fresno Cerezo, G. Rojo, F. Agulló-López, *J. Phys. Chem. B* **2000**, *104*, 43 – 47.
[12] N. F. Phelan, M. Orchin, *J. Chem. Educ.* **1968**, *45*, 633 – 637. It should be noted that this definition is not completely unambiguous since it can be interpreted to hold as well for linear π-conjugated systems.
[13] S. Fielder, D. D. Rowan, M. S. Sherburn, *Angew. Chem.* **2000**, *112*, 4501 – 4503; *Angew. Chem. Int. Ed.* **2000**, *39*, 4331 – 4333.
[14] M. R. Bryce, M. A. Coffin, P. J. Skabara, A. J. Moore, A. S. Batsanov, J. A. K. Howard, *Chem. Eur. J.* **2000**, *6*, 1955 – 1962.
[15] R. R. Tykwinski, *Chem. Commun.* **1999**, 905 – 906.
[16] Y. Zhao, R. McDonald, R. R. Tykwinski, *Chem. Commun.* **2000**, 77 – 78.
[17] M. Brønsted Nielsen, M. Schreiber, Y. G. Baek, P. Seiler, S. Lecomte, C. Boudon, R. R. Tykwinski, J.-P. Gisselbrecht, V. Gramlich, P. J. Skinner, C. Bosshard, P. Günter, M. Gross, F. Diederich, *Chem. Eur. J.* **2001**, *7*, 3263 – 3280.
[18] A. M. Boldi, J. Anthony, V. Gramlich, C. B. Knobler, C. Boudon, J.-P. Gisselbrecht, M. Gross, F. Diederich, *Helv. Chim. Acta* **1995**, *78*, 779 – 796.
[19] L. B. Brandsma, H. Verkruijsse, *Preparative Polar Organometallic Chemistry*, Springer, Berlin, **1987**, pp. 189 – 190.
[20] T. Imamoto, T. Kusumoto, M. Yokoyama, *J. Chem. Soc. Chem. Commun.* **1982**, 1042 – 1044.
[21] T. Imamoto, T. Kusumoto, M. Yokoyama, *J. Am. Chem. Soc.* **1989**, *111*, 4392 – 4398.
[22] A. Perrier-Datin, J.-M. Lebas, *J. Chim. Phys.* **1979**, *76*, 935 – 939.
[23] A. Bree, R. Zwarich, *J. Mol. Struct.* **1981**, *75*, 213 – 224.
[24] *Handbook of Chemistry and Physics*, 82nd ed. (Ed.: D. R. Lide), CRC, Boca Raton, FL, **2001**.
[25] I. Baraldi, E. Gallinella, M. Scoponi, *Spectrochim. Acta* **1987**, *43A*, 1045 – 1054.
[26] G. Varsányi, *Vibrational Spectra of Benzene Derivatives*, Academic Press, New York, **1969**.
[27] A. Perrier-Datin, J.-M. Lebas, *J. Chim. Phys.* **1979**, *76*, 925 – 933.
[28] Z. Meić, T. Šuste, G. Baranović, V. Smrečki, S. Holly, G. Kerestury, *J. Mol. Struct.* **1995**, *348*, 229 – 232.
[29] M. Oelgemöller, B. Brem, R. Frank, S. Schneider, D. Lenoir, N. Hertkorn, Y. Origane, P. Lemmen, J. Lex, Y. Inoue, *J. Chem. Soc. Perkin Trans. 2* **2002**, 1760 – 1771.
[30] B. Tian, G. Zerbi, K. Müllen, *J. Chem. Phys.* **1991**, *95*, 3198 – 3207.
[31] B. Tian, G. Zerbi, R. Schenk, K. Müllen, *J. Chem. Phys.* **1991**, *95*, 3191 – 3197.
[32] M. Del Zoppo, C. Castiglioni, P. Zuliani, G. Zerbi, in *Handbook of Conducting Polymers*, 2nd ed. (Eds.: T. A. Skotheim, R. L. Elsenbaumer, J. R. Reynolds), Marcel Dekker, New York, **1998**, pp. 765 – 822.
[33] It can not be ruled out that the ν_{8a} phenyl/phenylene C–C stretch mode contributes to the signal at 1603 cm^{-1}. It is anticipated that this mode is local in character and can not be held responsible for the observed superlinear dependence.
[34] G. Zerbi, E. Galbiati, M. C. Gallazzi, C. Castiglioni, M. Del Zoppo, R. Schenk, K. Müllen, *J. Chem. Phys.* **1996**, *105*, 2509 – 2516.
[35] D. R. Arnold, X. Du, J. Chen, *Can. J. Chem.* **1995**, *73*, 307 – 318.
[36] J. J. Apperloo, L. B. Groenendaal, H. Verheyen, M. Jayakannan, R. A. J. Janssen, A. Dkhissi, D. Beljonne, R. Lazzaroni, J.-L. Bredas, *Chem. Eur. J.* **2002**, *8*, 2384 – 2396.
[37] K. Meerholz, H. Gregorius, K. Müllen, J. Heinze, *Adv. Mater.* **1994**, *6*, 671 – 674.
[38] J. Roncali, *Acc. Chem. Res.* **2000**, *33*, 147 – 156.
[39] P. W. Fowler, P. Hansen, G. Caporossi, A. Soncini, *Chem. Phys. Lett.* **2001**, *342*, 105 – 112.
[40] K. Gustav, M. Boelke, *Z. phys. Chemie (Leipzig)* **1983**, *264*, 950 – 956.
[41] For noninteracting chromophores an increase of ε with n is also expected since, in that case, identical transitions are superpositioned. However, the PPP/SCF calculations indicate that it is indeed the HOMO – LUMO transition of the delocalized system which gains intensity.
[42] J. Cornil, D. Beljonne, C. M. Heller, I. H. Campbell, B. K. Laurich, D. L. Smith, D. D. C. Bradley, K. Müllen, J. L. Brédas, *Chem. Phys. Lett.* **1997**, *278*, 139 – 145.
[43] J. Michl, E. W. Thulstrup, *Tetrahedron* **1976**, *32*, 205 – 209.
[44] H. Meier, J. Gerold, H. Kolshorn, W. Baumann, M. Bletz, *Angew. Chem.* **2002**, *114*, 302 – 306; *Angew. Chem. Int. Ed.* **2002**, *41*, 292 – 295.
[45] N. Tyutyulkov, F. Dietz, K. Müllen, M. Baumgarten, S. Karabunarliev, *Chem. Phys.* **1994**, *189*, 83 – 97.
[46] PPP calculations on planar structures reveal the same trend as observed for the twisted structures. For planar **1** – **4**, calculated HOMO – LUMO transition energies are 4.89, 4.58, 4.60, and 4.66 eV, respectively, while the HOMO – LUMO gaps are 7.37, 6.85, 6.65, and 6.57 eV. This shows that the observed effects are not due to the nonplanar geometries of **1** – **4**.
[47] H. Hopf, *Angew. Chem.* **1984**, *96*, 947 – 958; *Angew. Chem. Int. Ed. Engl.* **1984**, *23*, 948 – 960.
[48] D. F. Eaton, *Pure Appl. Chem.* **1988**, *60*, 1107 – 1114.
[49] J. Griffiths, J. G. Lasch, QCPE Program QCMP054.
[50] J. J. P. Stewart, MOPAC, Version 7.0, 1993.
[51] R. H. Blessing, *J. Appl. Cryst.* **1997**, *30*, 421 – 426.
[52] A. Altomare, M. C. Burla, M. Camalli, G. L. Cascarano, C. Giacovazzo, A. Guagliardi, A. G. G. Moliterni, G. Polidori, R. Spagna, *J. Appl. Cryst.* **1999**, *32*, 115 – 119.
[53] G. M. Sheldrick, SHELXL-97, Program for Crystal Structure Refinement, University of Göttingen, Germany, 1997.
[54] A. L. Spek, Platon, a Multipurpose Crystallographic Tool, Utrecht University, The Netherlands, 2001.
[55] Beilstein Crossfire, Database BS0202AB, Beilstein Informationssysteme, 2002.

Received: December 16, 2002 [F4671]